JOURNAL OF MATERIALS SCIENCE 22 (1987) 46–56

The hygrothermal behaviour of glass fibre reinforced Pa66 composites: a study of the effect of water absorption on their mechanical properties

D. VALENTIN, F. PARAY, B. GUETTA
Ecole Nationale Supérieure des Mines de Paris, Centre des Matériaux, B.P. 87, 91003 Evry Cédex, France

A kinetic study of water absorption in three types of thermoplastic materials has been undertaken: pure Pa66 polymer, short fibre and continuous fibre composites. Ageing tests were carried out under nine sets of hygrothermal conditions: three different temperatures 40, 70, 90° C and three relative humidity levels, namely 30, 75 and 100% r.h. The results were found to obey a Fickian diffusion model and the characteristic parameters D (diffusion coefficient) and M_m% (maximum moisture content percentage) were determined. The influence of water uptake on residual mechanical properties was studied using three-point bending tests. For each type of composite, a water concentration threshold was detected beyond which a significant reduction in mechanical properties was observed.

1. Introduction

The rate at which the water is absorbed by a composite depends on many material variables. For instance the type of fibre and matrix, the fibre orientation with respect to the direction of diffusion, the temperature, the difference in water concentration between the composite and the environment and whether the absorbed water reacts chemically with the matrix.

Several studies have shown the important effects of absorbed water on the physical properties of composite materials [1–3]. However, to date the studies have mainly been concerned with thermoset matrix-based composites. It has been shown that above a threshold defined for a given temperature and relative humidity [4, 5] other mechanisms than simple diffusion can take place within the material; for example, plastification of the matrix or interfacial decohesion which leads to a degradation of the composite. It is therefore necessary to examine if such phenomena can occur for thermoplastic-based composites where, by definition, the plastification of the matrix is expected to be very important. It is also of prime interest to study how, for example, the glass transition temperature can play a role in the kinetics of water absorption.

2. Experimental techniques

A total of five materials were studied including the pure polymer Nylon 66, short and continuous glass fibre composite (Table I). All the composites were made by Peugeot SA (Audincourt, France). The volumic fraction was in the order of, respectively, 50% for material 1 (70% in weight) and 24% for material 2, 3, 4 (40% in weight). The length of the short fibres before elaboration was different for each material: from 0.2 to 0.5 mm for material 4, from 2 to 4 mm for material 3, and up to 9 mm for material 2. Since material 3 had a natural colour, material 2 was brown and material 4 was black due to the adding of black carbon.

The pure polymer and short fibre specimens were 160 mm long, 65 mm wide and 3 mm thick whereas continuous fibre specimens were 100 mm long, 37 mm wide for the same thickness, with the fibres aligned along the major axis.

Absorption tests were conducted in environmental chambers which allowed relative humidities in the range of 0 to 100% r.h. to be achieved for a range of temperature between 25 and 100° C. Relative humidity was controlled by using saturated salt solutions, the vapour pressure of which when in equilibrium with

TABLE I Main characteristics of the composite materials tested

Material	Fibre type	Source supplier	Fabrication technique	V_f	Matrix
0	Pure matrix	Rhône Poulenc	Injection moulding		Technyl A216
1	Continuous	IRCHA	Moulding	50%	Technyl A216
2	Short	IRCHA	Injection moulding		Technyl A216
3	Short	ICI	Injection moulding	24%	Maranyl
4	Short	Rhône Poulenc	Injection moulding	24%	Technyl A216

0022–2461/87 $03.00 + .12

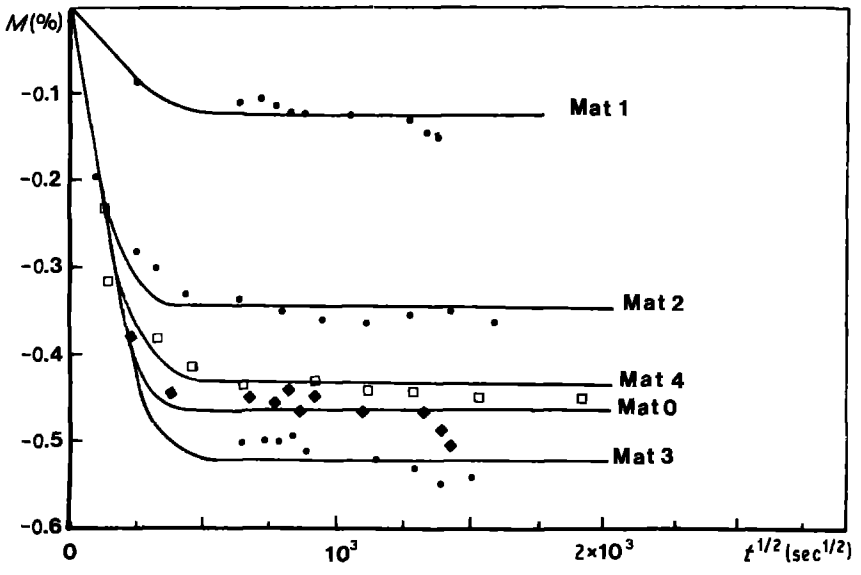

Figure 1 Weight loss of the different composites during drying.

the air gave very steady values [5]. Nine hygrothermal conditions were investigated: three temperatures 40, 70, 90° C and three relative humidities 30, 75 and 100% r.h.

Firstly the kinetics of water absorption were determined by weighing the specimens at regular intervals. A Sartorius balance type 1205 MP was used, with a precision of 1 mg. The balance was placed inside a Faraday cage in order to eliminate the influence of static electricity on the plates. The calculation of the coefficient of diffusion, D, and the maximum moisture content percentage M_m% was based on the experimental curve of weight gain as a function of time. For this, all materials were previously dried at 100° C and 0% r.h. in the presence of silica gel.

The residual properties after saturation, elastic moduli, E, in flexion and flexural failure stress, σ_R, were measured using a three-point bending test at room temperature. The samples were cut from the saturated plates and immediately tested. The dimension of the samples were equal to 15 mm × 60 mm with a span to depth ratio equal to 16. In addition, other bending tests on dried materials at different temperatures were also conducted by placing the bend test fixture in a climatic chamber. The temperature range covered was from −40° C to +140° C.

3. Kinetics of water absorption

The initial drying out of the different composites shows that the water content of these materials after fabrication was variable. A loss of the order of 0.1% was recorded for material 1, between 0.35 and 0.5% for short fibre composites, the moisture content of pure matrix was equal to 0.45% (Fig. 1). The behaviour during drying was Fickian: the curves of weight loss had two distinct parts, a linear part as a function of $t^{1/2}$ followed by a gradual dropping away until no moisture remained. However, a slight weight loss can be distinguished during the desorption phase which must be due to some permanent thermal ageing.

For temperatures equal to 40 and 70° C, a well-defined Fickian behaviour has also been observed both for the pure polymer and the composites. The general law for such behaviour can be written as [6]:

$$M\% = M_m\% \left\{1 - \frac{8}{\pi^2} \sum_{n=0}^{\infty} \left(\frac{1}{2n+1}\right)^2 \times \exp\left[-\frac{Dt}{h^2}\pi^2 (2n+1)^2\right]\right\} \quad (1)$$

where h is the thickness of the sample, M_m% the maximum moisture content, D the diffusion coefficient, and t the time.

The whole curve can be resolved into two parts described by two simple equations. The first part:

$$\frac{Dt}{h^2} \ll 0.05$$

$$M\% = M_m\% \frac{4}{\pi^{1/2}} \left(\frac{Dt}{h^2}\right)^{1/2} \quad (2)$$

which is the uptake of water by a semi infinitely thick specimen. The second part:

$$\frac{Dt}{h^2} > 0.05$$

which is described with the aid of the first term of the general Equation 1:

$$M\% = M_m\% \left\{1 - \frac{8}{\pi^2} \exp\left[-\frac{Dt}{2}\pi^2\right]\right\} \quad (3)$$

The parameters M_m% and D are calculated from the experimental points using Equations 2 and 3; a curve fitting techniques was used based on minimum variance which was developed for curves having an exponential form [7].

Knowing the diffusion parameter, D, and when a time–temperature equivalence exists, it is then possible to use the parameter $P = (Dt/h^2)^{1/2}$ in order to represent the curves for the materials. In that case, if the weight gain at saturation is only a function of the relative humidity, all the curves as a function of P, for a given relative humidity, are superimposed on a unique master-curve.

For temperatures below 90° C, this representation was accurate for all five materials (Fig. 2), since the

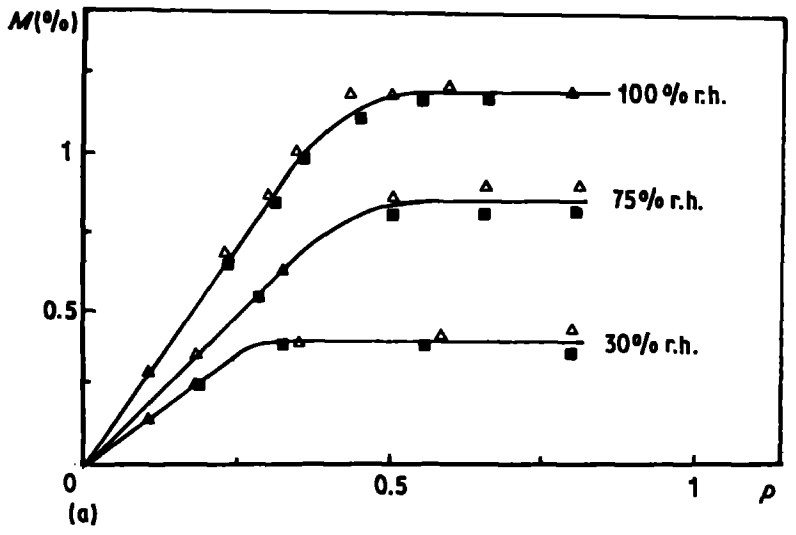

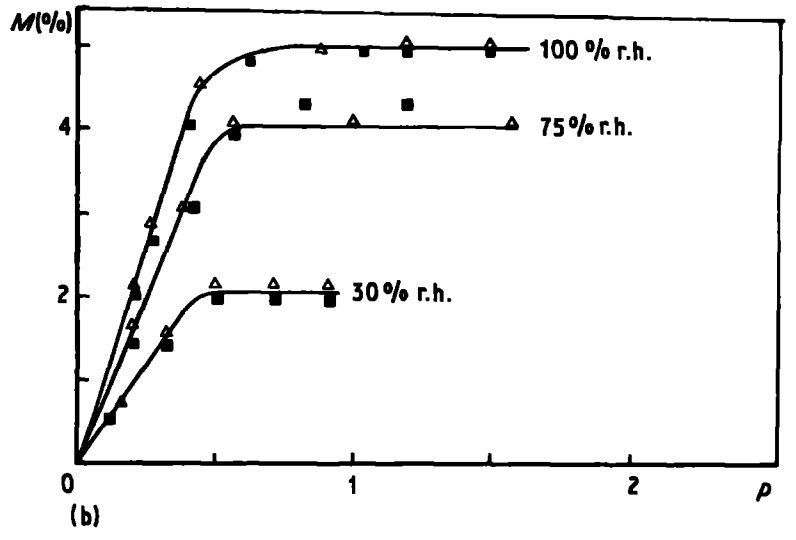

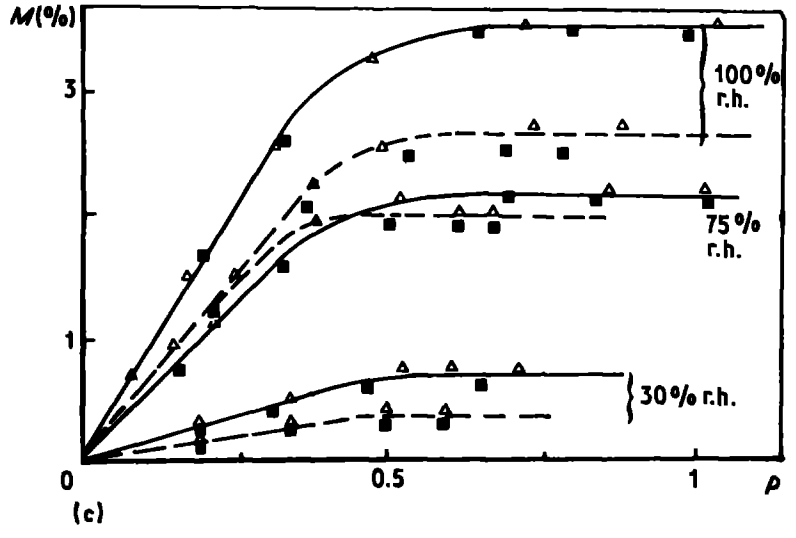

Figure 2 Absorption curves for (a) material 1, (b) pure polyamide, (c) materials 2 (– – –) and 3 (——), and (d) material 4. The weight gains were obtained at (△) 70° C and (■) 40° C.

diffusion parameters were only a function of temperatures (Fig. 3), following the classical Arrhenius-type law.

$$D = D_0 \exp - \frac{E_a}{RT} \quad (4)$$

where T is the temperature and E_a the activation energy, while the evolution of the saturation limits against relative humidity seems only to be a function of the relative humidity from the law:

$$M_m\,\% = a\,(\text{r.h. }\%)^b \quad (5)$$

with $b = 1$ for every material (Fig. 4).

Table II summarizes the data (D_0, E_a, a) obtained for the different conditions. The values of the activation energies are of the same order as those obtained

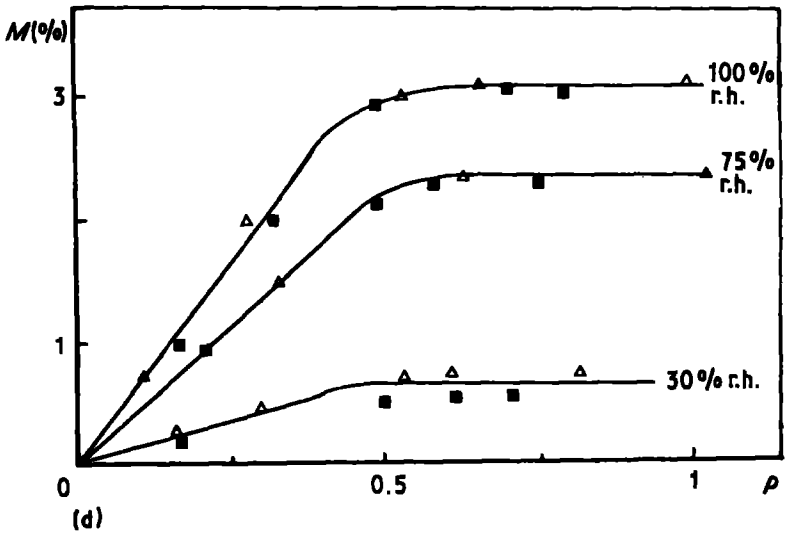

Figure 2 Continued.

with thermoset matrix composites (12.5 kcal mol^{-1}). On the other hand, the values of coefficients of diffusion obtained on material 1 (continuous fibres) are greater than those obtained on unidirectional epoxy-based composites [5, 8].

Above 70° C, a weight loss was observed on the pure nylon specimen and with material 1 during ageing at 30% r.h. (Fig. 5), whereas the amount of absorbed water at 75% r.h. was nearly twice as much as that at 100% r.h. for the short fibre composites and for the pure matrix (Fig. 4). The same tendancy, but less pronounced, is observed for material 1. It must be added that at 100% r.h. and for short fibre composites, an "oscillation" around an equilibrium point is observed that should really be the steady linear plateau of the saturation curve. However, no anomalies in the values of the diffusion coefficients which have been calculated at 90° C (Fig. 3) can be seen, although the coefficients calculated at 100° C, during drying, are greater than predicted.

From the amount of absorbed water on pure matrix $M_m\,\%_m$ knowing the volume fraction of the reinforcement, the theoretical amount of absorbed water in the composite $M_m\,\%_c$ can be deduced:

$$\frac{M_m\,\%_c}{M_m\,\%_m} = \frac{\varrho_m}{\varrho_c}(1 - V_f) \qquad (6)$$

where ϱ_m and ϱ_c are, respectively, the densities of the matrix and the composite. The ratio given in Equation 6 is equal to 0.6 for materials 2, 3, 4 and equal to 0.3 for material 1. It can be seen from Table III that the experimental values are always lower than the theoretical ones except at 100% r.h. at 40 and 70° C for the short fibre composites. The experimental ratio is closer to the theoretical one at the higher relative humidity. For long fibre composites, the same tendency is observed but to a lesser extent. These results are surprising if they are compared with those obtained on thermoset composites where the theoretical values are often lower than the experimental ones [9]. The difference is explained by the role played by the fibre–matrix interface.

Another significant ratio can be calculated and compared to experimental results:

$$\frac{M_m\,\%_{CF}}{M_m\,\%_{LF}} = \frac{\varrho_{LF}}{\varrho_{CF}}\frac{(1 - V_{fCF})}{(1 - V_{fLF})} = 2 \qquad (7)$$

where CF and LF correspond, respectively, to short fibre and long fibre composites. The main interest of such a calculation, consists in shunting the values obtained on pure matrix and only taking into account

TABLE II Values of energy of activation E_a, and parameters a and D_0 for the different materials

Material	E_a(kcal mol^{-1})	D_0(mm^2 sec^{-1})	a
0	12.5	325	5×10^2
1	12.5	130	1×10^{-2}
2	12.5	400	2.6×10^{-2}
3	12.5	400	3.1×10^{-2}
4	12.5	400	3×10^{-2}

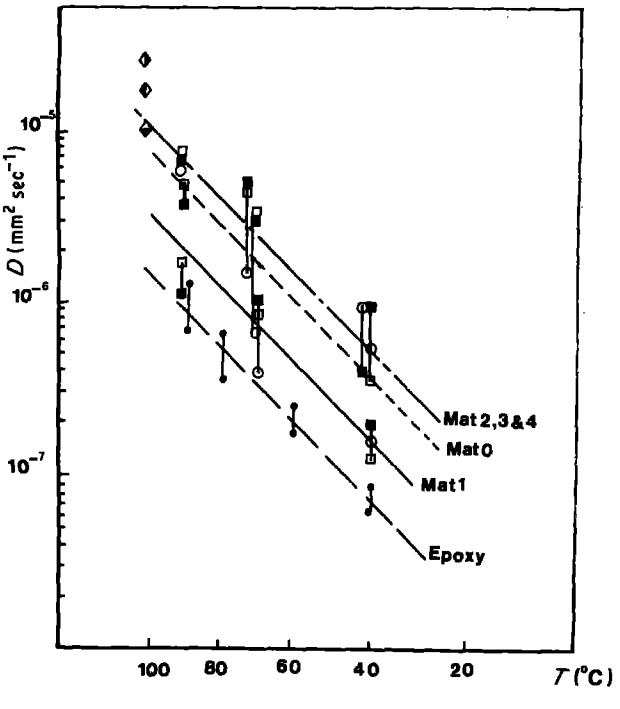

Figure 3 Diffusivity against temperature for the different materials tested. The values have been compared with an epoxy-based composite [5]. (■) 100% r.h., (□) 75% r.h., (○) 30% r.h. Drying tests: (◆) materials 2, 3 and 4, (◆) material 0, (◆) material 1.

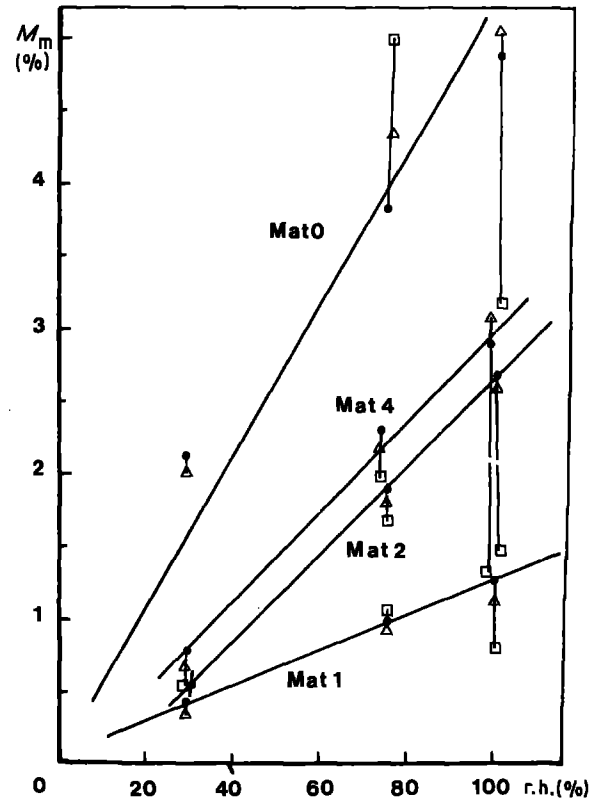

Figure 4 Saturation limits against relative humidity for the different materials. The water uptake at 90° C and 100% r.h. is less important than expected for every composite. (●) 70° C, (△) 40° C, (□) 90° C.

those results obtained on composites in the event that the matrix undergoes some structural change during fabrication. It can be seen from Table III that the experimental results are greater than the theoretical predictions except for the three following conditions: 30% r.h. at 40 and 70° C and 100% r.h. at 90° C. Fibres may obstruct the absorption of water and this all the more as their volume fraction is important and the relative humidity is low. The results obtained at 90° C are apart from this behaviour.

The same approach can be made with the coefficient of diffusion, D. For continuous fibres, the transverse coefficient can be written as [10]:

$$D_{\perp} = D_m \left[1 - 2\left(\frac{V_f}{\pi}\right)^{1/2}\right] \quad (8)$$

Since, for short fibre composites, the coefficient of diffusion, D_{CF}, lies between two bounds, D_{UB} and D_{LB}, UB and LB stand, respectively, for upper and lower bounds [11] with:

$$D_{UB} = \tfrac{2}{3} D_{\perp} + \tfrac{1}{3} D_L \quad (9)$$

$$D_{LB} = \left(\tfrac{2}{3} D_{\perp}^{-1} + \tfrac{1}{3} D_L^{-1}\right) \quad (10)$$

where D_L and $D_{\perp}$ are the longitudinal and transverse coefficients of diffusion of a continuous fibre composite having the same volume fraction. Then:

$$D_L = D_m (1 - V_f) \quad (11)$$

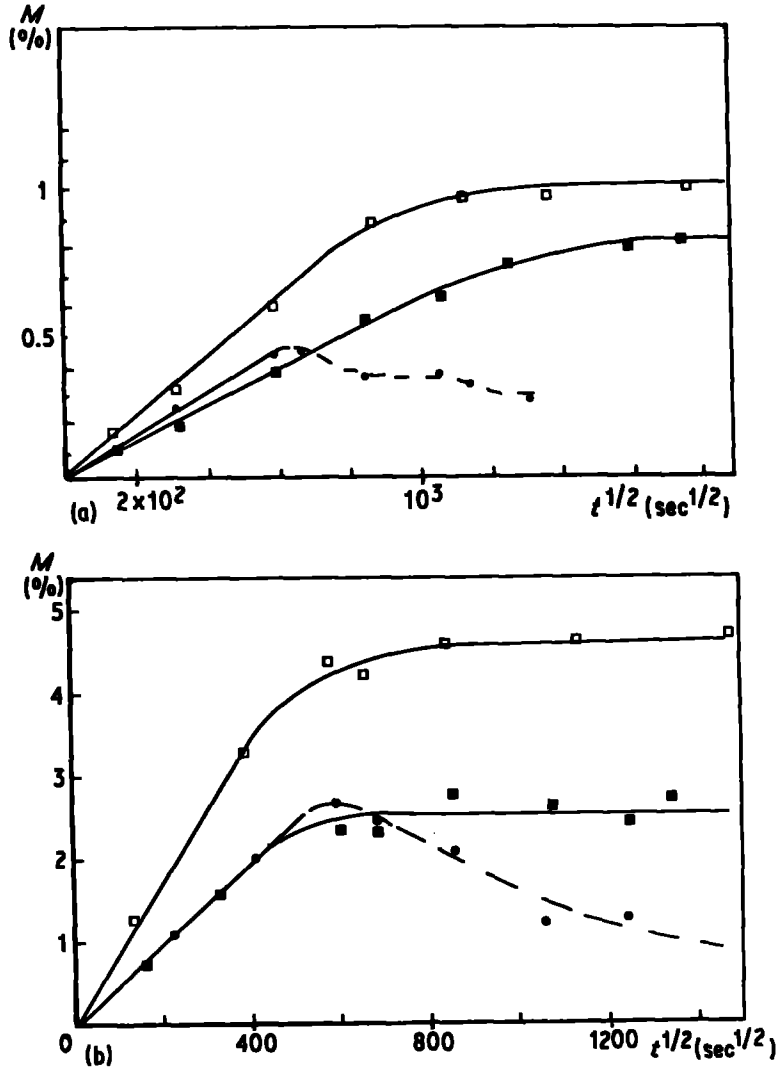

Figure 5 Absorption curves for (a) material 1, (b) pure polyamide, (c) materials 2 (——) and 3 (– – –), and (d) material 4, at 90° C. In this case the use of parameter p to describe the behaviour is not accurate. (■) 100% r.h., (□) 75% r.h., (●) 30% r.h.

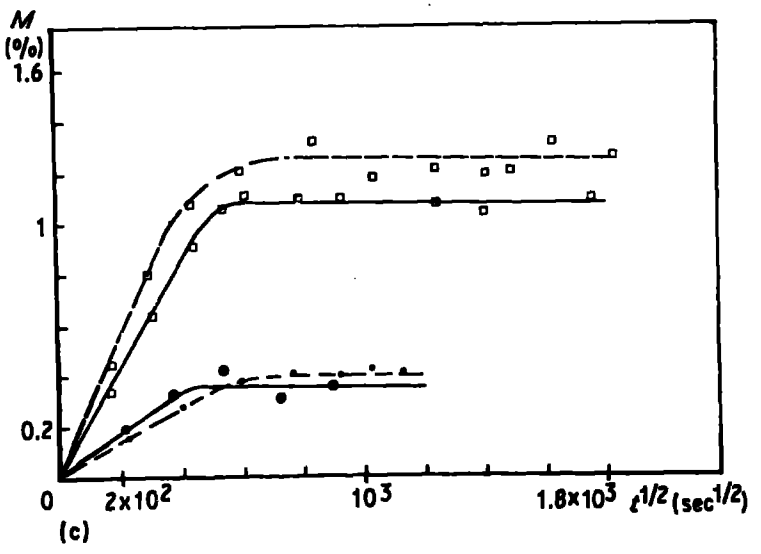

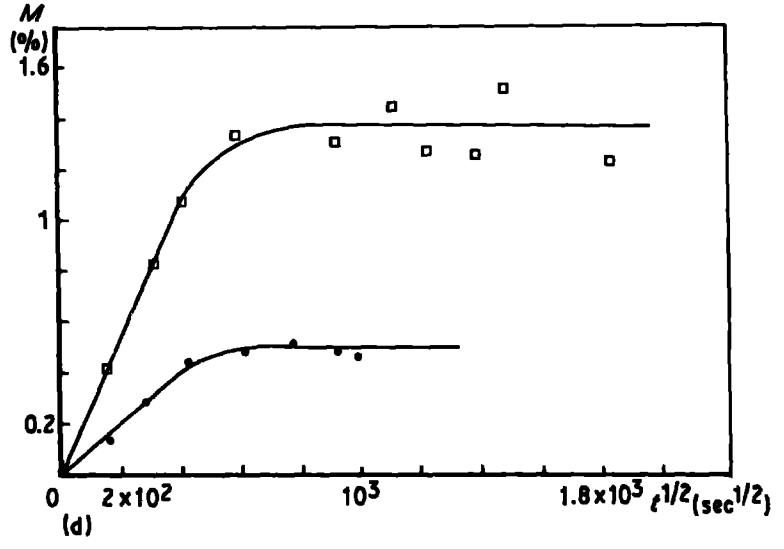

Figure 5 Continued.

TABLE III Values of the experimental ratio of weight gain as a function of the hygrothermal conditions

	Temperature (°C)								
	40			70			90		
	30% r.h.	75% r.h.	100% r.h.	30% r.h.	75% r.h.	100% r.h.	30% r.h.	75% r.h.	100% r.h.
$\frac{M_m\%_{CF}}{M_m\%_m}$	0.25	0.52	0.58	0.30	0.55	0.62	–	0.31	0.48
$\frac{M_m\%_{LF}}{M_m\%_m}$	0.17	0.19	0.25	0.2	0.2	0.24	–	0.2	0.28
$\frac{M_m\%_{CF}}{M_m\%_{LF}}$	1.42	2.4	2.5	1.5	2.34	2.54	–	1.5	1.8

TABLE IV Experimental values of the coefficient of diffusion for short and continuous fibres compared to those obtained on pure matrix

	Temperature (°C)								
	40			70			90		
	30% r.h.	75% r.h.	100% r.h.	30% r.h.	75% r.h.	100% r.h.	30% r.h.	75% r.h.	100% r.h.
$\frac{D_\perp}{D_m}$	0.34	0.38	0.2	0.6	0.22	0.33	–	0.32	0.25
$\frac{D_{CF}}{D_m}$	2.2		0.36	2.5	0.9	0.9	–	1.2	1.84
$D_\perp$ (mat. 1) 10^{-6} mm²sec^{-1}	0.17	0.14	0.2	0.36	0.9	1.2	–	1.7	1
D_{CF} (mat. 3) 10^{-6} mm²sec^{-1}	0.7		0.5	1.1	4	4.6	5.85	6.7	9

TABLE V Percentage weight loss after the second drying compared to the first one

	Temperature (° C)					
	40			70		
	30% r.h.	75% r.h.	100% r.h.	30% r.h.	75% r.h.	100% r.h.
Mat. 2	0.1	0.1	0.12	0.1	0.15	0.2
Mat. 3	0.02	0.04	0.08	0.07	0.18	0.24
Mat. 4	–	–	–	0.014	0.023	0.034

TABLE VI Evolution of the percentage of crystallinity as a function of the hygrothermal history. All samples have been redried before DSC analysis

Conditions	Mat. 1	Mat. 2	Mat. 4
Dried	34.6	28.5	39.1
70° C, 30% r.h.	44.2	–	–
70° C, 75% r.h.	–	27	43.2
70° C, 100% r.h.	–	33	44.8
90° C, 30% r.h.	47.8	35	–

TABLE VII Values of coefficient B and stress at rupture at −40° C for the different materials tested

Material	$\sigma_R(T_0)$ (MPa)	B ($10^{-3}K^{-1}$)
1	1100	5.5
2	290	2
3	325	3
4	250	1.8

and $D_\perp$ is determined from Equation 8 with $V_f = 24\%$. It can be deduced that the theoretical ratio $D_\perp/D_m$ is equal to 0.2 and D_{CF}/D_m is lower than 0.54 and higher than 0.51. Table IV summarizes the experimental results. It can be seen that the theoretical ratios are always overstepped. The diffusion coefficients are all the greater, for a given temperature, the higher the relative humidity. (Table IV and Fig. 3).

A second drying after ageing at 70° C shows that the absorbed water is linked to a reversible phenomenon since it was possible to a large extent, to return to the critical weight after the first drying. However, the final weights are generally slightly below the initial values after drying, the short fall being a function of relative humidity (Table V). As the period of initial drying was identical for every sample, as was the period of hygrothermal ageing and of the second drying. The differences cannot be explained by simple thermal ageing. It must be concluded that water uptake has led to leaching of the samples.

Some physical transformation of the materials cannot be excluded for thermoplastics, also a structural evolution has been undertaken by DSC. As a matter of fact, it is well known that a crystalline polyamide will absorb less water than an amorphous polyamide [12], therefore hygrothermal ageing should modify somewhat the structure of the matrix and hence some results could not be justifiably comparable. It can be seen (Table VI) that a certain increase of the crystallinity is detected during the ageing. The increase is greater when the temperature is higher but also when the relative humidity is higher. However, these variations do not exceed 10%, which do not invalidate the results concerning composite weight gains.

4. Mechanical tests

4.1. Effect of temperature

Bending tests were performed on dried materials in the range of temperature between −40 and +140° C. The evolution of the stress at rupture as well as the elastic modulus was examined.

Failure stress was seen to obey the following

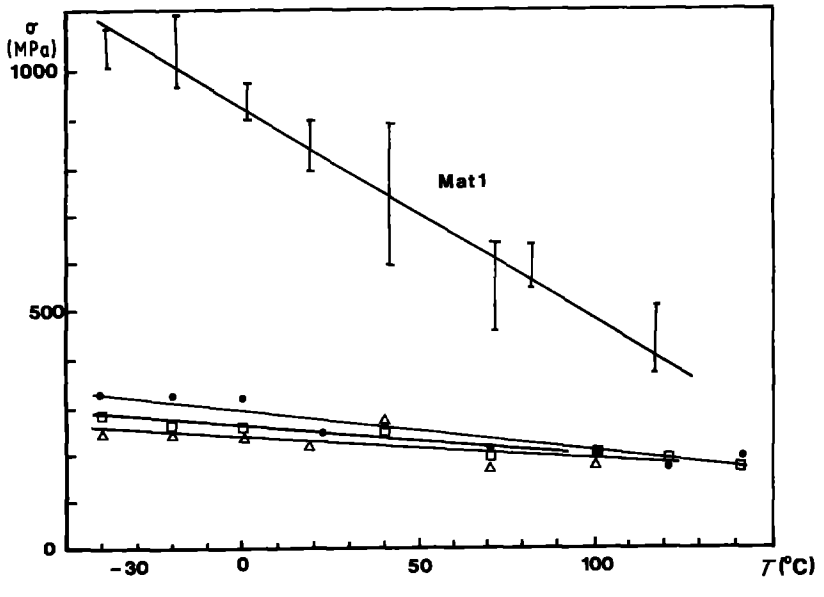

Figure 6 Variation of stress at rupture in flexion as a function of temperature for the different materials tested. (●) Material 2, (□) material 3, (△) material 4.

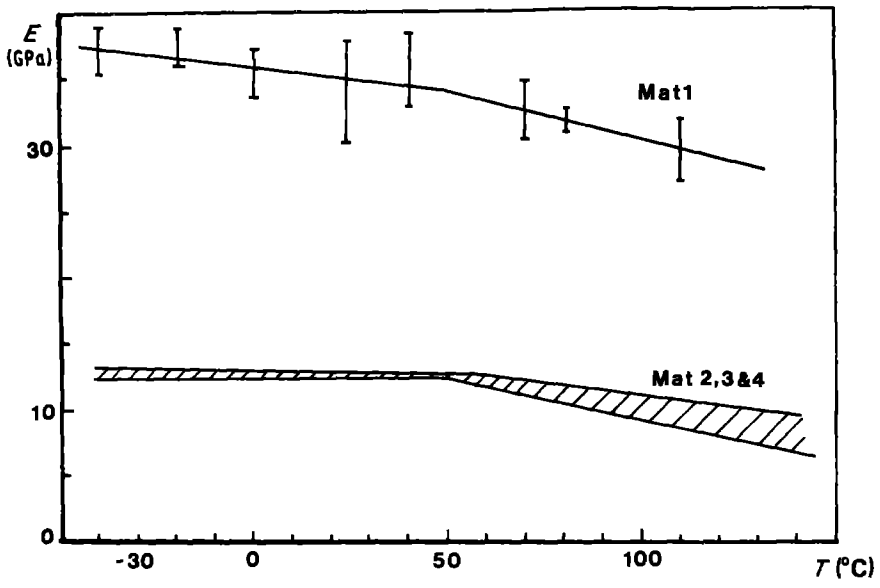

Figure 7 Variation of the flexural modulus as a function of temperature for the different materials tested.

equation as a function of temperature:

$$\sigma_R(T) = \sigma_R(T_0)\,[1 - B(T - T_0)] \quad (12)$$

where B is a coefficient, T is the temperature and σ_R is the stress at rupture at $-40°$ C. However, the relative fall, and therefore coefficient B, is more important for continuous fibres (Fig. 6). For short fibre composites, the relative fall is more important when the stress at rupture at $-40°$ C, that is to say σ_R (T_0), is higher (Table VII). The use of relatively long fibres (up to 9 mm) for material 4, did not improve the mechanical properties of the composite significantly. The long fibres could have been broken during the elaboration of the composites. We can deduce the value of the glass transition temperature, about 55° C, above which a drop can be distinguished (Fig. 7) and a plastification of the matrix can be observed (Figs 8 and 9) from the evolution of the elastic modulus, for all the composites.

4.2. Effect of humidity

The mechanical properties in flexion at room temperature of saturated composites have been compared with those obtained on dried materials.

A noticeable effect of water appears only for quantities higher than 1% for materials 2, 3 and 4, as well as for elastic moduli or stress at rupture (Figs 10a and b). As shown in Figs 10b, c, the threshold is at a lower value for material 1 (0.5%) and the greatest drop is relatively less important than for short fibre composites (33% instead of 50%). These different thresholds are to be compared with those obtained on epoxy-based composites (0.6%) [5]. However, in general, the mechanisms involved are different in so much as the

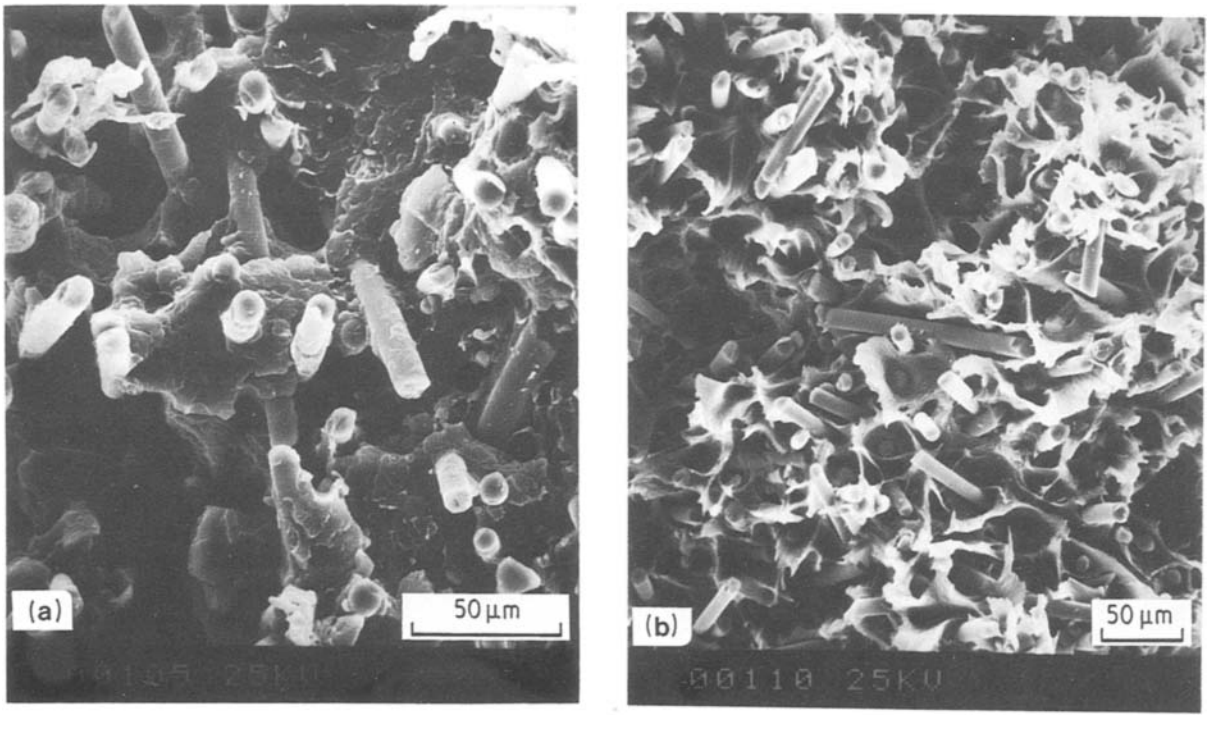

Figure 8 Scanning electron micrographs of the fracture surface of material 4 obtained in flexion at (a) $-40°$ C and (b) 100° C, showing the plastification of the matrix.

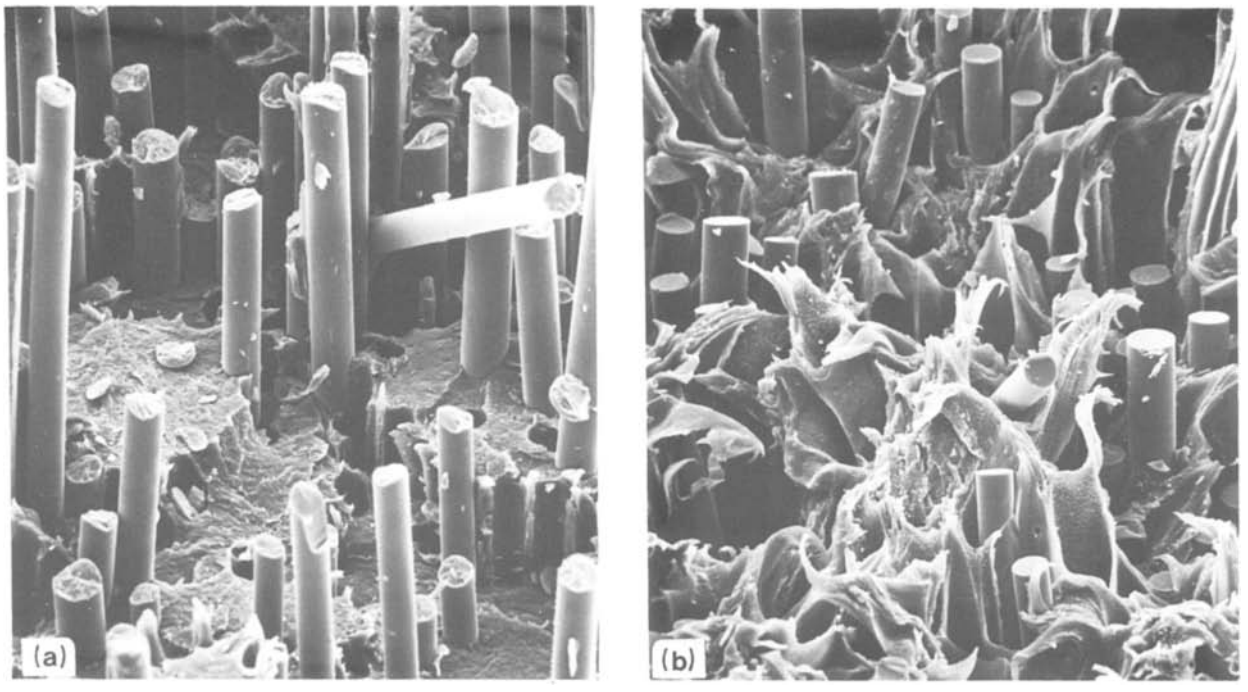

Figure 9 Scanning electron micrographs of the fracture surface of material 1 at (a) −40° C and (b) 100° C. The fracture surface of the matrix is brittle at −40° C.

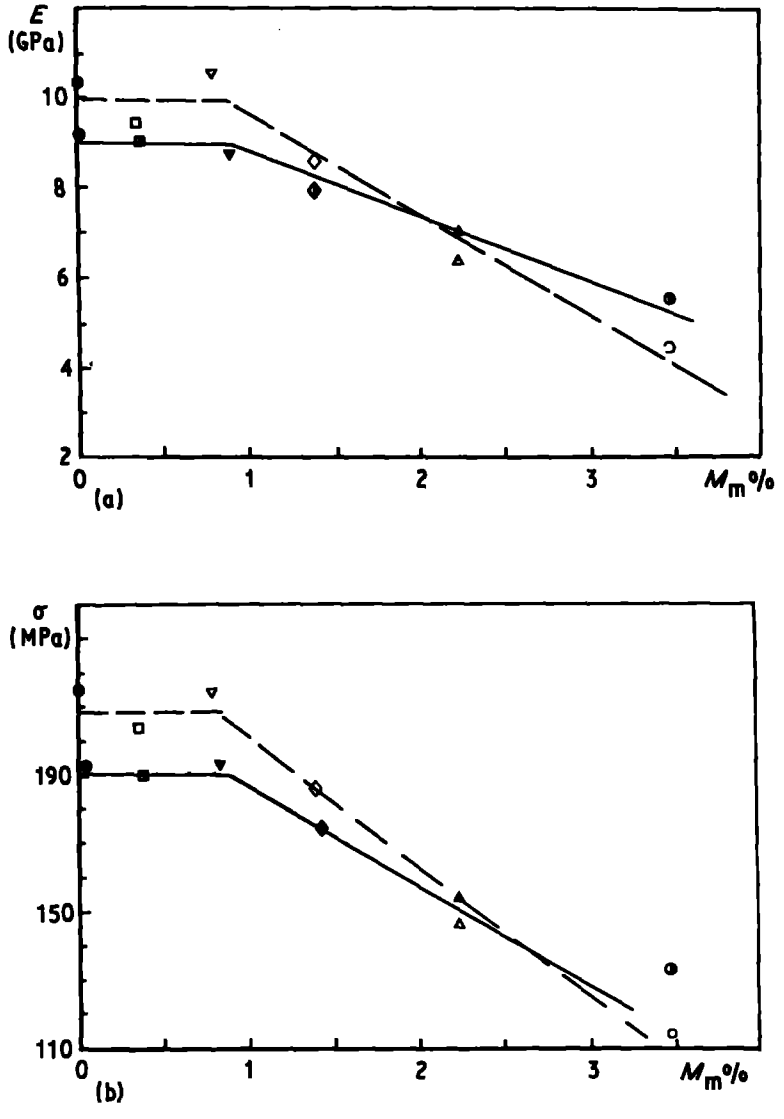

Figure 10 Variation of stress at rupture, and elastic modulus as a function of maximum water uptake for material 1 (c and d) and materials 3 (——) and 4 (– –) (a and b). (▽, ○, △) 70° C, (◇, □) 90° C.

Figure 10 Continued.

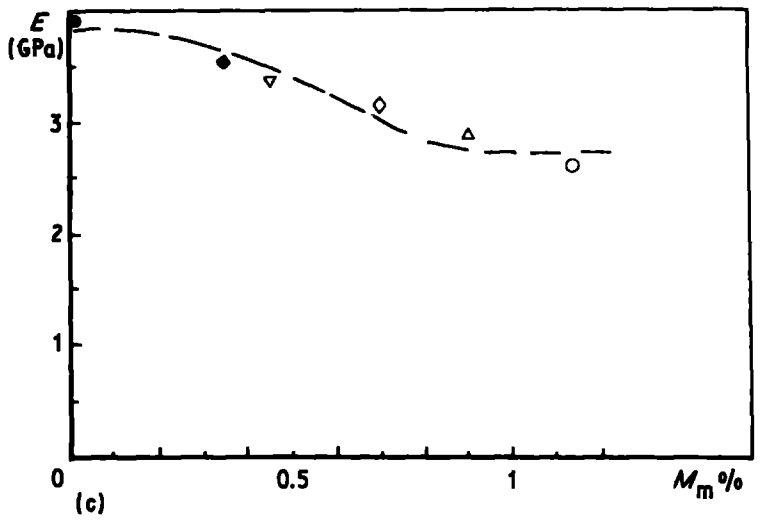

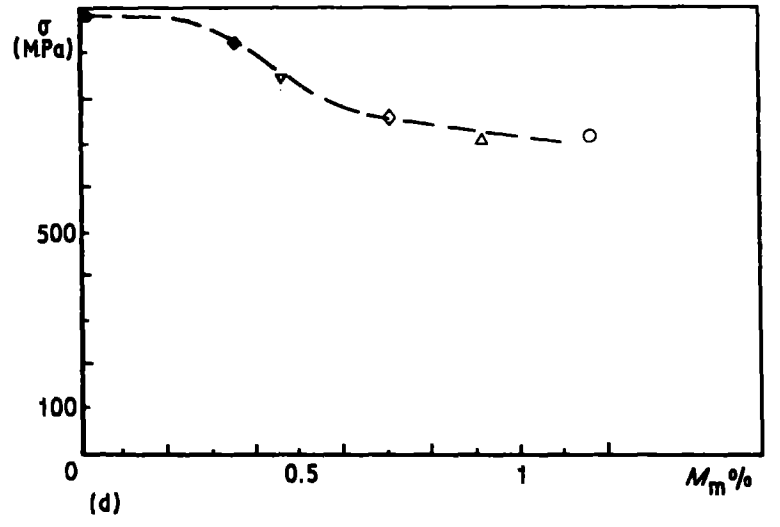

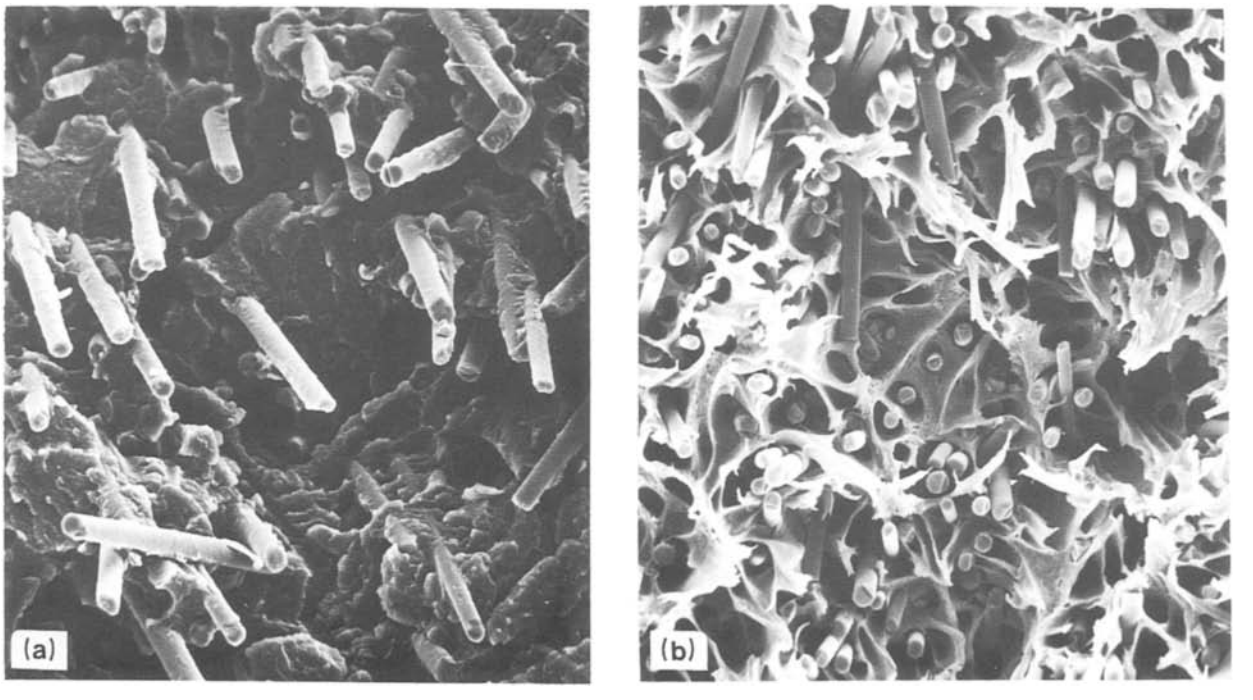

Figure 11 Scanning electron micrographs of (a) the fracture surface of material 4 after drying, compared to (b) the surface obtained after 39 days ageing at 70° C and 100% r.h.

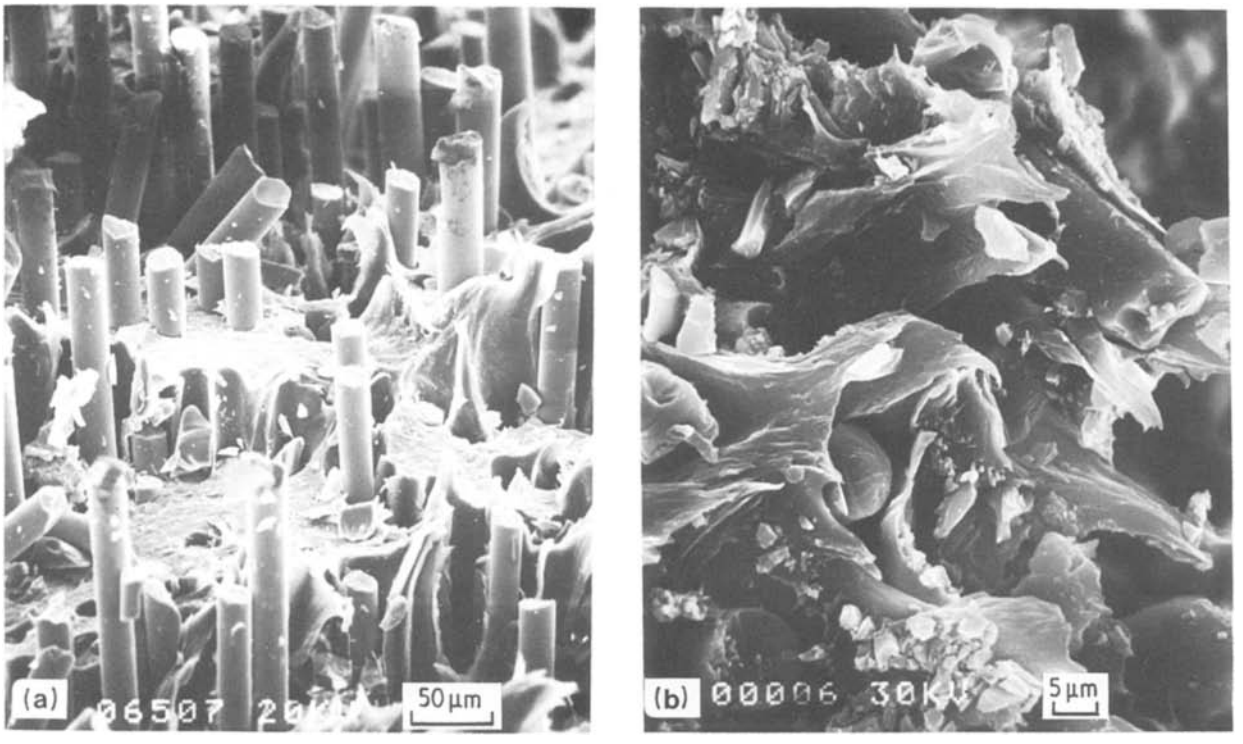

Figure 12 Comparison of fracture surfaces obtained on material 1 in (a) the tension part and (b) in the compression part of the samples. The flexion test was performed after 39 days of ageing at 70° C and 100% r.h.

role played by the fibre–matrix interface was preponderant. Here, the main consequence of the water uptake is a plastification of the matrix (Fig. 11). This plastification is more extensive the greater the amount of water uptake. For continuous fibres, this plastification is more visible in part of the sample in compression rather than in tension (Fig. 12).

5. Conclusions

The hygrothermal behaviour of Pa66 glass fibre composites seems to be relatively different from thermoset composites.

For temperatures below or equal to 70° C, Fick's law can be applied to describe the phenomenon but some divergences arise in the coefficient of diffusion, for example.

At higher temperature, other mechanisms operate, such as thermal ageing, oxidation and leaching, which disturb the behaviour.

The water uptake leads to a shift of the glass transition temperature of the matrix. The greater drop in mechanical properties of short fibre composites is due to the higher resin loads compared to their long fibre counter part. (This behaviour is observed for a proportionally lower quantity of absorbed water.)

Acknowledgements

The authors would like to thank the Ministere de la Recherche et de l'Industrie for their financial support and also Peugeot SA and IRCHA for their collaboration during this study.

References

1. C. M. SHEN and G. S. PRINGER, *J. Compos. Mater.* **11** (1977) 2.
2. *Idem, ibid.* **11** (1977) 250.
3. D. ISHAI and V. ARNON, "Instantaenous effect of internal moisture conditions on strength of glass reinforced plastics", Advanced Composite Materials, Environmental Effects. ASTM STP 658 (American Society for Testing and Materials, Philadelphia, Pennyslvania, 1978) pp. 267–76.
4. B. DEWIMILE and A. R. BUNSELL *Composite* **14** (1983) 34.
5. P. BONNIAU and A. R. BUNSELL, Water Absorption by Glass Fibre Reinforced Epoxy Resin, in "Composite Structures", edited by I. H. Marshall (Applied Science, London, 1981) pp. 92–105.
6. J. CRANK, "The Mathematics of Diffusion" (Claredon Press, Oxford, 1956) p. 42.
7. D. LEVIS III, *Ceram. Bull.* **57** (1978) 151.
8. A. C. LOOS and G. S. SPRINGER, *J. Compos. Mater.* **3** (1979) 131.
9. B. DEWIMILLE and A. R. BUNSELL, *J. Phys. D Appl. Phys.* **15** (1982) 2079.
10. G. S. SPRINGER and S. W. TSAI, *J. Compos. Mater.* **1** (1967) 166.
11. C. W. BERT and R. A. KLINE, *Polym. Compos.* **6** (1985) 133.
12. "Encyclopedia of Polymer Science and Technology", Vol. 10, (Interscience, New York).

Received 29 November 1985
and accepted 4 March 1986